



Designing Modified Graphene Oxide-epoxy Coatings for Enhancing the Corrosion Resistant Performance of Mild Steel in Sodium Chloride Solution

N. THAMARASELVI* and D. NALINI

Department of Chemistry, PSGR Krishnammal College for Women,
Coimbatore, Tamil Nadu, India.

*Corresponding author E-mail: thamaraikumaran2012@gmail.com

<http://dx.doi.org/10.13005/ojc/380619>

(Received: November 02, 2022; Accepted: December 30, 2022)

ABSTRACT

An eco-friendly, graphene oxide-based nanofiller was synthesised for epoxy resin coating. The behaviour of nanofiller on mild steel against corrosion was evaluated in this study. Graphene oxide synthesised by Hummer's method was treated with an ethanol extract of *Boerhaavia diffusa* (BD) plant leaves. GCMS was used to identify the phytochemicals present in BD. Grapheneoxide treated with BD (GO-BD) and GO were examined by FT-IR and FE-SEM. The corrosion behaviour of the neat epoxy, epoxy containing GO, and GO-BD was determined by electrochemical studies in 3.5 wt% sodium chloride solution. Surface changes of the coated substrates were analysed by a peel-off test, a salt spray test, and a static water contact angle measurement. Results showed that the modified graphene oxide sheets act as excellent filler for epoxy coated mild steel panels in a 3.5 wt% sodium chloride medium.

Keywords: Modified GO sheets, 3.5% sodium chloride, Electrochemical studies, Salt spray test, Peel-off measurement and static contact angle.

INTRODUCTION

Corrosion is a serious problem that causes failure of the equipment and surface damage to the metals. It also causes economic losses¹⁻³. It cannot be eliminated completely. But it can be reduced by the addition of inhibitors⁴⁻⁷ (organic and inorganic) to the corrosive media, alloying⁸⁻⁹, and surface coatings¹⁰⁻¹². Surface coatings may be polymer coatings, metallic coatings, or non-metallic coatings. A polymer coating protects the metal by acting as a barrier between the metal and the environment.

Epoxy resin is widely used in polymer coatings due to its excellent adhesion and corrosion resistance properties. The epoxy coating has good mechanical and thermal properties and low shrinkage. While curing, it produces many pores and microcracks due to its poor impact resistance and high brittleness. Hence, prolonged exposure to corrosive media causes hydrolytic degradation. This acts as a path for the electrolyte ions to create corrosion. In order to enhance the protection performance of polymer coatings with nanofillers, pigments were added. Yong Zing *et al.*, developed silicon nitride dispersed epoxy



resin enhanced by organosilanes and evaluated the performance of corrosion protection and adhesion strength on Q235 carbon steel¹³. Kartsonakis *et al.*, examined the barrier performance of epoxy coatings modified with ceramic nanocontainers filled with inhibitors, water traps, and chloride¹⁴. The anticorrosion performance of nickel rGO-TiO₂ composites for mild steel in various acids was evaluated by Kh. El. Sayed, *et al.*,¹². For the past few years, graphene oxide nanofillers have played a vital role in corrosion studies. Peimin Hou *et al.*, investigated the corrosion resistance and barrier performance of a graphene oxide nanocontainer in carbon steel encapsulated with polymeric ionic liquid¹⁵. A composite of graphene oxide and zeolite was developed by B.M. Daas *et al.*,¹⁶, and the inhibition ability of the composite on aluminium corrosion in alkaline solution was evaluated by weight loss and tafel plots. Shengguo *et al.*, designed an epoxy zinc rich coating embedded with GO and rGO. Electrochemical measurements were adopted to study the anticorrosion behaviour of the coating on a steel substrate¹⁷. Ali Asghar Javid Parvar *et al.*, investigated the corrosion inhibition and protection behaviour of a Ce-GO pigmented epoxy polyamide coating on steel¹⁸. Recently, graphene oxide and functionalized graphene oxide were introduced to enhance epoxy coatings against corrosion. According to the literature, GO-based nanofillers demonstrate superior barrier performance. Hence, the present study is focused on enhancing the anti corrosion property of epoxy coating on mild steel substrates using GO and modified GO nanofillers. For this study, graphene oxide was synthesised and modified with plant extract. The mild steel substrate was coated with neat epoxy resin and epoxy resin treated with nanofillers (GO, GO-BD). The coated mild steel substrate was subjected to potentiodynamic polarization, EIS, peel testing, salt spray testing, and wettability measurement in order to measure the corrosion inhibition, strength, water adsorption, and stability of the coating.

EXPERIMENTAL

Materials

A fresh and mature *Boerhaavia diffusa* plant was collected from Kalapatti village, Coimbatore. All of the chemicals and solvents were purchased and used from Sigma Aldrich. The mild steel (0.01% S, 0.01% N, 0.02% P, 0.2 % Mn, 0.09% carbon, and

99.67% iron) and epoxy resin (density 0.96 g/cm³) and hardener were purchased in Coimbatore district.

Synthesis of graphene oxide

Graphene is oxidised to graphene oxide (Hummer's method)¹⁹⁻²¹. 25 mL of sulfuric acid were slowly added to 0.5 g of graphite powder. The mixture was constantly stirred for two hours. Then 0.3 g of sodium nitrate was added little by little, and the temperature was reduced to 0°C. 3 g of potassium permanganate was added gradually, and the temperature of the mixture was kept at less than 20°C. Then the contents of the vessel were transferred to a water bath maintained at 35°C and stirred for half an hour. 170 mL of deionised water was added to the mixture, and then 5 mL of hydrogen peroxide was added. The black mixture turned brown. Then it was centrifuged, filtered, and rinsed with 4% hydrochloric acid. Then the resulting residue was repeatedly washed with distilled water, to get rid of impurities. The prepared GO was examined by FT-IR to confirm the oxidation of graphite, and then FE-SEM analysis was also performed.

Preparation of plant extract

The *Boerhaavia diffusa* plant was selected to modify GO. The plant belongs to the Nyctaginaceae family. The plant leaves were collected in Coimbatore, Tamil Nadu, India. About 80 g of fresh and healthy leaves were chosen and thoroughly washed with water. The washed leaves were cut into small pieces. Then the leaves were transferred to a container, and about 250 mL of ethyl alcohol was added. The container was sealed tightly and kept for 24 hours. The plant extract was filtered and used for further study. The plant extract was characterised by GCMS and FT-IR.

Treatment of BD extract with GO

2 g of GO was added to 120 mL of deionized water and then sonicated. After 10–15 min of sonication, 80 mL of BD extract was mixed. A magnetic stirrer was used for thorough mixing, and then it was centrifuged. The resulting residue was filtered and washed with deionized water. Therefore, unreacted free molecules were removed. The residue was dried and labelled as GO-BD, used for characterization and coating.

Graphene Oxide/GO-BD and epoxy composite preparation

2 g of GO and GO-BD were separately added to 10 mL of distilled water. Next, the mixtures were separately sonicated for 10 min for a better

dispersion. Then 30 g epoxy resin and 6 mL of dimethyl formamide were added to each container. Then the resin and (GO/GO-BD) mixture was sonicated for 20 min, resulting in the transfer of GO and GO-BD particles from the aqueous phase to the resin phase (wet transfer).

Preparation of various epoxy coatings

Mild steel substrates were abraded with 600, 800, and 1200 grit silicon carbide paper and degreased with acetone. Neat epoxy resin was applied on pretreated mild steel substrate, which was used as a reference. Epoxy treated with GO-BD and epoxy treated with graphene oxide applied to mild steel. Coated substrates allowed drying for a day at room temperature and 3 h at 100°C in a hot air oven. The thickness of the coating was 0.055 mm.

Characterisation of BD, GO-BD and, GO

Organic compounds present in plants were detected by GCMS (Agilent GCMS analyzer). Fourier transform-IR analysis was used to expose the structure of the BD, GO and GO-BD. FT-IR was performed with a wavenumber range of 4000-400 cm^{-1} (using a Shimadzu spectrometer). Micrographs of GO sheets and GO treated with BD were analysed by FESEM (ZEISS instrument).

In NaCl solution, electrochemical impedance and potentiodynamic polarisation studies on mild steel substrates were carried out. The neat epoxy, GO-epoxy, and GO-BD/epoxy-coated substrates were immersed in the 3.5 wt.% sodium chloride solution. EIS and polarisation tests were carried out with NOVA Auto lab at different time intervals. In this study, a three-electrode cell namely a saturated calomel electrode, a platinum electrode, and coated mild steel substrates, was used. The impedance and polarisation measurements were performed at OCP in the frequency range of 100 kHz to 10 mHz.

The salt spray test was carried out in a salt spray chamber. It was performed according to ASTM B 117:2019. The surface changes of the various epoxy-coated substrates were examined using 4 cm x 5 cm mild steel substrates. A sharp knife was used to produce an artificial defect on the coated panels. Coated substrates were placed at a 45° angle in a salt spray cabin that was kept at 35±2°C and pH 6.5 to 7.2°C, respectively. A sodium chloride solution (5%wt) was continuously sprayed on the mild steel substrate for 300 hours. The changes on the mild steel substrates were noticed every 24 hours.

The contact angle was used to determine wettability. The measurements were carried out using the system model OCA²⁰. The angle of contact and shape of a water drop placed on the coated metallic surface were measured at room temperature. For this, a single water drop is placed on the surface of the coated mild steel substrates. The nature of the water drop was recorded after 10 seconds using a Canon digital camera.

The adhesive strength value of coated mild steel substrates was measured using a Peel tester. In this test, a polymer tape was adhered to the coated substrate. A constant force was applied at an angle of 90° to peel the coating. All the coated substrates were subjected to this test, and the force required to peel the coating was measured.

RESULTS AND DISCUSSION

Characterisation of GO and GO-BD

IR spectrum received for the GO-BD and GO is exposed in Fig. 1. It was an evidence for the structural changes in GO by BD leaf extract. The absorption of the -OH moiety results in a broad peak at 3435 cm^{-1} in the IR spectra of GO. A peak seen at 1614 cm^{-1} , 1031 cm^{-1} , and 1232 cm^{-1} , owing to C-C skeletal vibration and C-O-C in the epoxide group. The absorption frequency identified at the frequency range of 1703 cm^{-1} and 1390 cm^{-1} was due to CO stretching vibration. CH₂ peaks were observed in the range of 2854 cm^{-1} (symmetric) and 2999 cm^{-1} (asymmetric). A medium and weak peak at 1452 cm^{-1} was consistent with the existence of an aromatic ring. The spectrum of GO-BD shows the absorption associated with both BD plant leaf extract and GO. This established BD absorption on the surface of GO and that GO was modified.

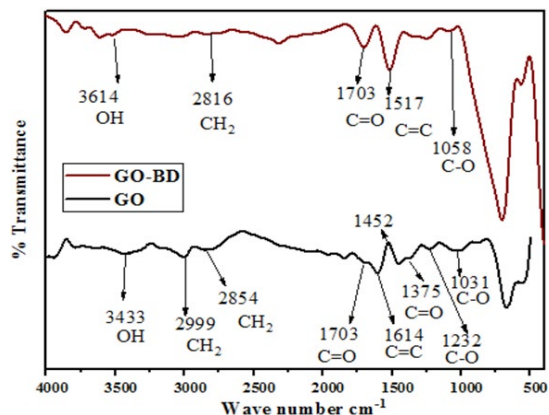
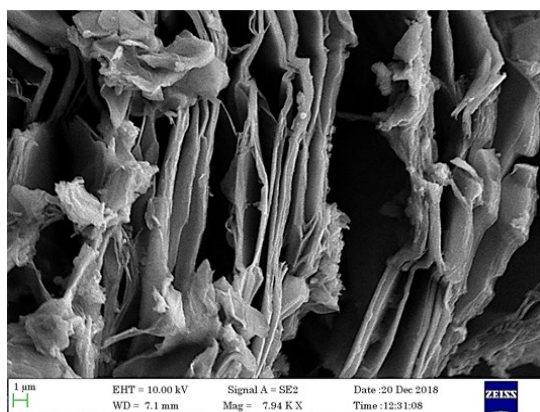
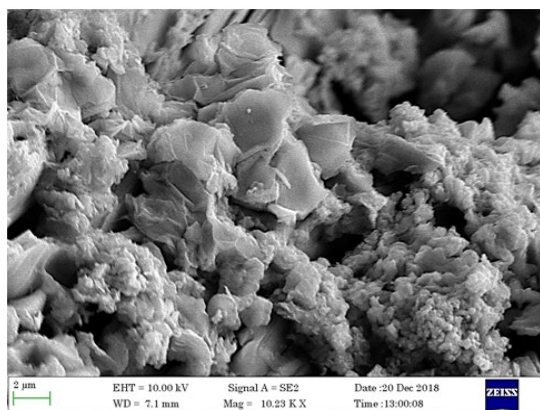


Fig 1 . FTIR spectrum of GO and GO-BD

The ethanol extract of the plant was subjected to Gas Chromatography–Mass Spectroscopy. From the results, many organic compounds were identified. Some of them are (a) 1-Adamantane carboxylic acid, 2-phenyl ethyl ester, (b) Pyridine, 3-ethyl-5-methyl-, (c) 1,4 Dioxane-2,3-diol, diacetate, (d) 1H-Purine-2,6,8,(3H)-trione, 7, 9-dihydro-1,3dimethyl-. The modification of GO sheets by the plant extract was also analysed by SEM. Fig. 2 a and b show images of graphene oxide, GO-BD, that show multiple layers that were observed in the graphene oxide micrograph. The micrograph of GO-BD totally varied from GO. GO-BD shows a rough surface and a folded morphology. It is clear from the results that leaf extract modified the structure of graphene oxide.



(a)



(b)

Fig. 2. FESEM images of (a) GO, (b) GO-BD

Salt spray test

Figure 3 shows the images of mild steel substrates coated with untreated epoxy, epoxy treated with GO, and epoxy treated with GO-BD. a1,

b1, and c1 were the images of the substrates before exposure to 5% sodium chloride, and then they were exposed for 300 hours continuously. Substrates were observed every 24 hours. Photographs of mild steel panels after 300 hours were displayed in a2, b2, and c2. Results clearly indicate that rust formed after 144 and 300 hours at the x-marked area. As the exposure period increases, the amount of the corrosion product also increases. However, in the case of GO-BD/epoxy, the corrosion products are lower than in neat epoxy, GO-epoxy. Corrosion products in the x-marked area may be due to the dissemination of the corrosive agents.

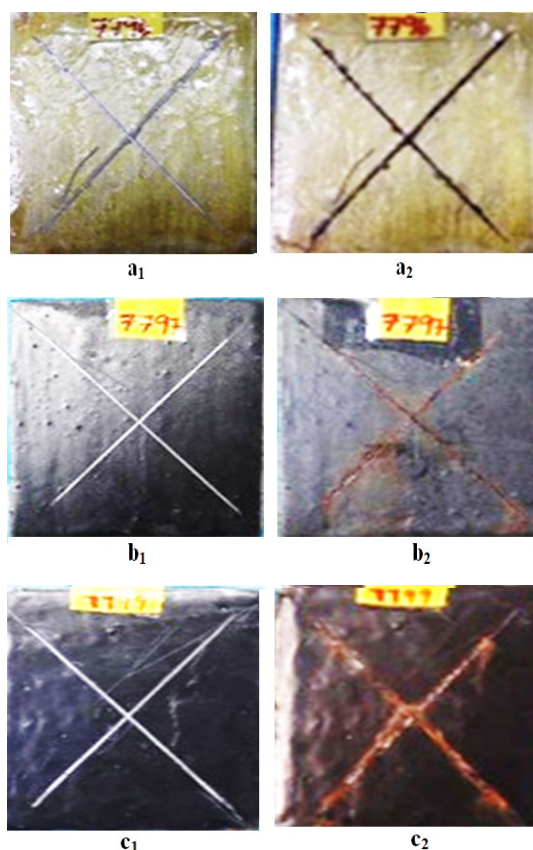


Fig. 3. Salt spray test images of mild steel substrate (a1) neat epoxy (b1) epoxy treated with GO and (c1) GO-BD/epoxy before exposure and (a2) neat epoxy (b2) epoxy treated with GO and (c2) GO-BD/epoxy 300 h exposure

Contact angle measuring method

The wetness of the metal substrate is determined by the contact angle value of a surface. This was measured to determine how well epoxy coatings protect against corrosion. The plain epoxy coated mild steel's contact angle value was determined to be 74.5°. Epoxy/

GO and epoxy/GO-BD had contact angles of 78.7° and 91.3°, respectively. Substrates, those coated with neat epoxy and those covered with epoxy/GO, had a contact angle value less than 90 degrees. It demonstrates the coating's hydrophilic properties²²⁻²⁸. When compared to neat epoxy and epoxy-GO, the substrate coated with epoxy/GO-BD had a higher contact value. This demonstrated the mild steel substrate's limited wetting ability under an epoxy/GO-BD coating. Low wettability indicates inadequate electrolyte infiltration into the coated surface interface.

Electrochemical impedance measurements

OCP values of neat epoxy, epoxy treated GO, and GO-BD/epoxy applied mild steel engrossed in 3.5 wt% sodium chloride at different time periods were measured, and the values are listed in Table 1. It is clear from the table that as the immersion time extends, the OCP value shifts towards a negative value. Penetration of the electrolyte into the metal/coating boundary is the main reason for the shift in OCP. The value was higher in the GO-BD-filled epoxy coating than in the other two coatings. This indicates enhanced barrier performance of GO-BD. OCP against immersion time plots are displayed in Fig. 4. In order to study the anticorrosion behaviour of epoxy treated GO and GO-BD, electrochemical impedance was performed with a 3.5% sodium chloride solution. Fig. 5. shows the Nyquist plot of mild steel substrates coated with neat epoxy, epoxy treated with GO, GO-BD/epoxy. The electrochemical impedance parameters, namely charge transfer resistance (R_{ct}), coating resistance (R_c), and total resistance (R_t), fitted with two time constants, are listed in Table 2. Results clearly indicate that as immersion time increases, coating resistance decreases for the three coated substrates, proving the entry of aqueous sodium chloride into the coating or metal barrier. After 24 h of immersion, the R_t values of neat epoxy, epoxy treated with GO, GO-BD/epoxy coated substrates all decreased. The decrease in the R_t value was due to the entry of the corrosion ions into the metal coating barrier. At 3 days immersion, the R_t value

of GO-BD/epoxy is significantly higher than that of the other coatings. This is due to the inhibitory effect of the GO-BD molecules present in the coating.

Table 1: OCP values of potentiodynamic polarization of substrates immersed in 3.5 wt% NaCl solution at various time periods

Sample	Immersion time	OCP vs SCE
Epoxy	Initial	-0.5059
	1hour	-0.62091
	Day 1	-0.55815
	Day 3	-0.5839
GO /Epoxy	Initial	-0.36448
	1hour	-0.54387
	Day 1	-0.62791
	Day 3	-0.63085
GO-BD/Epoxy	Initial	-0.43898
	1hour	-0.54075
	Day 1	-0.5605
	Day 3	-0.59199

Table 2: Impedance parameters extracted from electrochemical studies

Sample	Immersion Time	R_{ct} (ohmcm ²)	R_c (ohmcm ²)	R_t (ohmcm ²)
Epoxy	Initial	457	3037	3494
	1hour	249	2761	3010
	1 day	36.5	219	255.5
	3 day	23.6	150	173.6
GO/Epoxy	Initial	6770	1660	8430
	1hour	4000	965	4965
	1 day	1870	519	2389
	3 day	586	189	775
GO-BD/Epoxy	Initial	76600	10900	87500
	1hour	48000	7730	55730
	1 day	14200	3210	17410
	3 day	9970	1410	11380

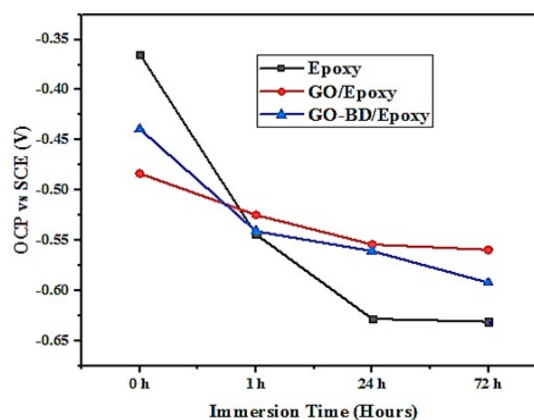


Fig. 4. OCP plots against exposure time for (a) neat epoxy (b) epoxy treated with GO (c) GO-BD/epoxy at different time intervals

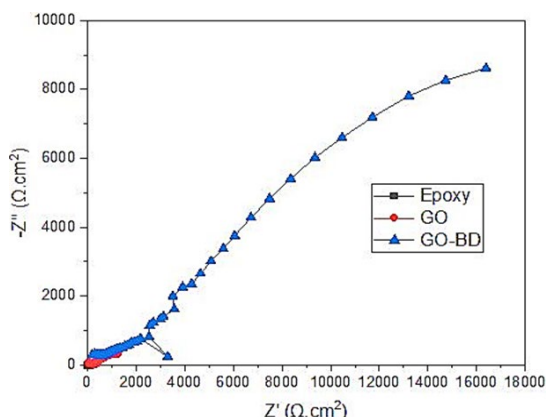


Fig. 5. Nyquist plots for neat epoxy, epoxy treated with GO, GO-BD/epoxy coatings after 3 days of exposure to 3.5% NaCl

To investigate the protection mechanism, a polarisation test was performed. Electrochemical parameters i_{corr} , E_{corr} , β_a , β_c were collected from Tafel extrapolation technique and the outcome are listed in Table 3. From Fig. 6. both anodic and cathodic current altered towards low current densities with the addition of GO-BD/epoxy. i_{corr} value of the epoxy coated, GO/epoxy and GO-BD/epoxy mild steel was $1.86E^{-06}$ $\mu A/cm^2$, $1.61E^{-06}$ $\mu A/cm^2$ and $1.28E^{-07}$ $\mu A/cm^2$ at the time of exposure to 3.5% NaCl. i_{corr} value of GO-BD epoxy was low compared to GO/epoxy and neat epoxy coated mild steel substrate. Addition of GO-BD shows a low i_{corr} value than the other two coatings. This shows the protection behaviour of the modified GO/epoxy on mild steel substrate.²⁹⁻³⁹

Table 3: Potentiodynamic polarization parameters of mild steel samples immersed in 3.5 wt% NaCl at different time intervals

Time	Sample	b_a (V/dec)	b_c (V/dec)	E_{corr} (V)	i_{corr} ($\mu A/cm^2$)
initial	Epoxy	0.15328	0.1257	-0.39203	1.86E-06
	Epoxy/GO	0.14603	0.28978	-0.55183	1.61E-06
	Epoxy/GO-BD	0.37418	0.22119	-0.46475	1.28E-07
1 Hour	Epoxy	0.11374	0.33576	-0.6319	5.29E-06
	Epoxy/GO	0.14944	0.23554	-0.58497	2.63E-06
	Epoxy/GO-BD	0.17347	0.17848	-0.59198	1.95E-07
Day 1	Epoxy	0.08761	0.11678	-0.64804	7.63E-05
	Epoxy/GO	0.21597	0.30508	-0.59912	8.68E-06
	Epoxy/GO-BD	0.14888	0.26386	-0.62385	6.97E-07
Day 3	Epoxy	0.06617	0.08425	-0.66166	1.32E-05
	Epoxy/GO	0.2399	0.1928	-0.58759	2.22E-05
	Epoxy/GO-BD	0.083392	0.11922	-0.65856	4.10E-07

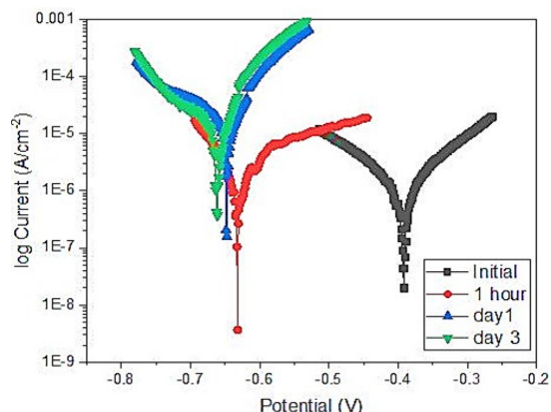


Fig. 6a. Potentiodynamic polarization plots of neat epoxy coated mild steel immersed in 3.5% NaCl solution

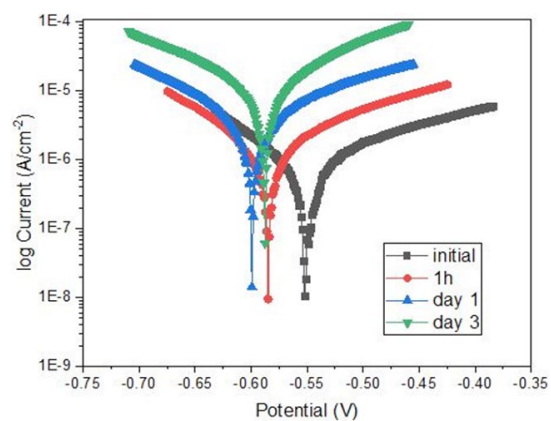


Fig. 6b. Potentiodynamic polarization plots of epoxy treated with GO coated mild steel immersed in 3.5% NaCl solution

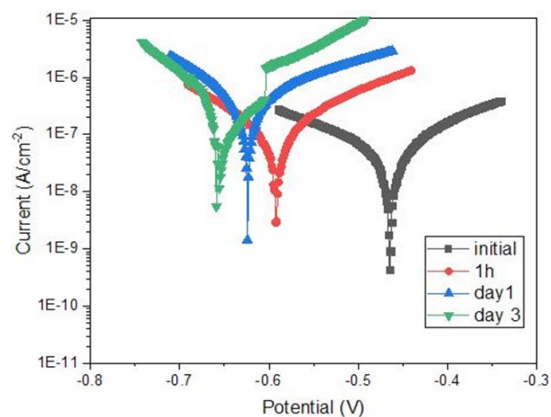


Fig. 6c. Potentiodynamic polarization plots for GO-BD/epoxy coated mild steel immersed in 3.5% NaCl solution

Peel test measurements

The peel-off test determined the force required to debond the coating. Load vs displacement plots are displayed in Fig. 7. Peel strength value of the GO-BD/epoxy coating was

found to be 1.478N. The strength of GO-BD/ epoxy composite coating was better than the neat epoxy and epoxy treated with GO coating⁴⁰. This showed that GO-BD increased the strength of the coating.

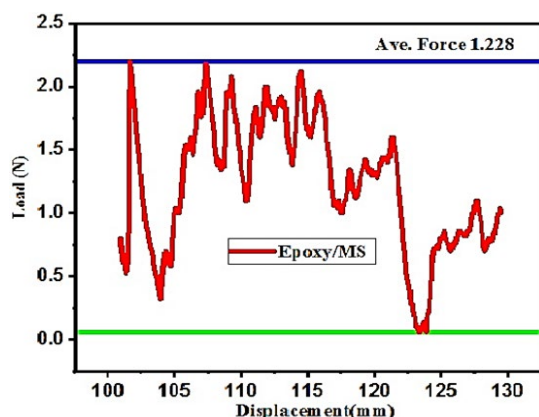


Fig. 7a. Displacement Vs Load plots of neat epoxy coated mild steel substrate

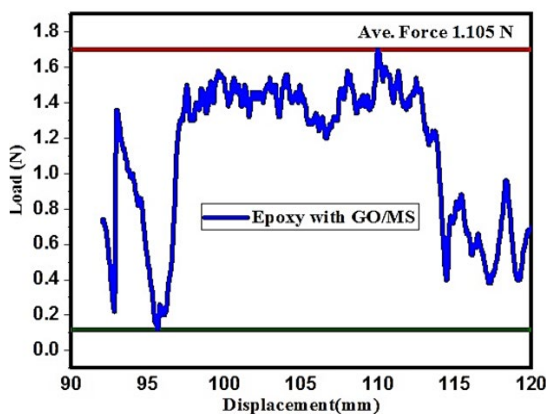


Fig 7b. Displacement Vs Load plots of GO/epoxy coated mild steel substrate

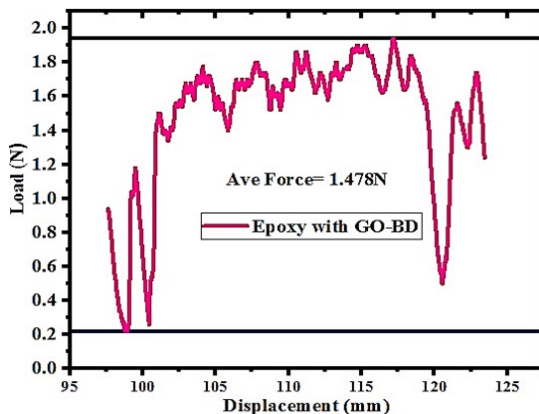


Fig 7c. Displacement Vs Load plots of GO-BD/epoxy coated mild steel substrate

Protection mechanism of the epoxy coatings

Micropores and other flaws are created during the application and/or curing processes of an epoxy coating on a steel surface. Electrolytes may diffuse into the coating medium in this manner, degrading the coating. The coating delaminates when the electrolyte gets to the coating/metal interface. Failure of the coating is caused by the development of a water film at the polymer/steel interface. Strong hydrogen bonds are created between polar epoxy resin groups and water molecules, which are powerful hydrogen bonding agents. When there is a water film present, the hydrogen bonds that exist between the polar epoxy groups and the hydrated oxide coating on the steel surface may be compromised. More electrolytes may diffuse over time and start corrosion processes at the coating/metal interface. Due to the numerous polar oxygen-containing groups (COOH and OH) found in GO films, which are incompatible with epoxy resins, pure GO films have a high hydrophilicity. As to the agglomeration of the GO sheets, the coating matrix develops flaws and voids. New channels for electrolyte diffusion into the coating matrix are opened up by agglomerated GO films. Because of the GO layer's high propensity for water molecules, electrolyte diffuses more readily into the coating matrix, and the coating's effectiveness as a barrier suffers. The epoxy matrix's addition of graphene oxide particles lengthens the electrolyte diffusion path. The epoxy matrix and dispersion stability of GO are both improved by surface treatment. Polar groups of epoxy can interact with GO-BD particles. The plant *Boerhaavia diffusa* may functionalize GO sheets, which could lessen the particles' hydrophilicity. Ions, oxygen, and water cannot pass through GO-BD plates. By creating zigzag diffusion channels, the GO-BD particles fill holes, flaws, and free epoxy volumes, making the coating less permeable. Electrolyte migration into the coating matrix and coating/metal interface can be greatly decreased in the presence of GO-BD foils. Less coating deterioration and coating delamination are the results. Another method for enhancing coating protection performance is the impact of GO-BD on epoxy/steel interfacial adhesion. The epoxy and steel substrate can adhere more tightly and steadily by using GO-BD.

CONCLUSION

FT-IR and FESEM results reveal that successful oxidation of graphite and modification of GO sheets by *Boerhaavia diffusa* leaves.

Leaf extract improved the hydrophobic nature and adhesive strength of the coatings on mild steel substrate.

Electrochemical studies and Salt spray

test showed the anticorrosion behaviour and barrier performance of GO-BD/epoxy composite coating against corrosive medium.

Peel test is an evidence for the improved strength of the composite coatings.

ACKNOWLEDGEMENT

Authors are grateful to PSGR Krishnammal College for women for the essential amenities provided.

REFERENCES

- Dwinanda, R.P.; Haryoko, A. F.; Kurnia, J. C. *Mater. Today Pro.*, **2020**, *46*, 1699–1704.
- Liu, X.; Chen, L.; Liu, Z.; Song, Q.; Liu, C. *Nanotechnol. Rev.*, **2021**, *10*, 1236–1252.
- Chaouiki, A.; Lgaz, H.; Zehra, S.; Salghi, R.; Chung, I.M.; Yasmina El Aoufir, Y. E.; Subrahmanya Bhat, K., Ali, I. H.; Gaonkar, S.L.; Mohammad I. Khan.; Oudda, H. *J. Adhes. Sci. Technol.*, **2019**, *33*, 921–944.
- Ameh, P. O.; Ukoha, P. C. *Ind. Chem.*, **2016**, *2*, 27–35.
- Baig, N.; Chauhan, D. S.; Saleh, T. A.; Quraishi, M. A. *New J. Chem.*, **2019**, *43*, 2328-2337.
- Singh, G.; Arora, S. K.; Tripathy, A.; Dochania, M. *J. Integr. Sci. Technol.*, **2016**, *4*, 76–80.
- Salman, T.; Al-Amiery, A. A.; Shaker, L. M.; Kadhum, A. A. H.; Takriff, M. S. *Int. J. Corros. Scale Inhib.*, **2019**, *8*, 1035–1059.
- Huang, X.; Ke, R.; Dong, Y. *J. Sol-Gel Sci. Technol.*, **2020**, *94*, 671–680.
- Fotovvati, B.; Namdari, N.; Dehghanhadikolaei, A. *J. Manuf. Mater. Process.*, **2019**, 3doi: 10.3390/jmmp3010028.
- Xu, H.; Hu, H.; Wang, H.; Li, Y.; Li, Y. R. *Soc. Open Sci.*, **2020**, *7*, doi: 10.1098/rsos.191943.
- Zhang, K.; Lu, J.; Li, J.; Zhang, D.; Gao, L.; Zhou, H. *Corros. Sci.*, **2020**, *164*, 108352.
- El-Sayed, K.; Hamid, Z. A.; Salah Eldin, T. A.; Khalil, M. W.; Hassan, H. B. *J. Mater. Environ. Sci.*, **2019**, *10*, 141–162.
- Zhang, Y.; Zhao, Z.; Zhang, J.; Shao, Q.; Li, J.; Li, H.; Lin, B.; Yu, M.; Chen, S.; Guo, Z. *J. Polym. Res.*, **2018**, *25*, doi: 10.1007/s10965-018-1518-2.
- Kartsonakis, I.A.; Athanasopoulou, E.; Snihirova, D.; Martins, B.; Koklioti, M.A.; Montemor, M.F.; Kordas, G.; Charitidis, C.A. **2014**, *Corr. Sci.*, <http://dx.doi.org/10.1016/j.corsci.2014.04.009> 0010-938.
- Hou, P.; Liu, C.; Wang, X.; Zhao, H. *Int. J. Electrochem. Sci.*, **2019**, *14*, 3055–3069.
- Daas, P.M.; Ghosh, P. K.; Ghosh, S. *Indian J. Sci. Technol.*, **2017**, *10*, 1–11.
- Zhou, Y.; Wu, Y.; Zhao, W.; Yu, J.; Jiang, F.; Wu, Y.; Ma, L. *Mater. Des.*, **2019**, *169*, 107694.
- Javidparvar, A. A.; Naderi, R.; Ramezanzadeh, B. *Compos. Part B Eng.*, **2019**, *172*, 363–375.
- Gerani, K.; Mortaheb, H. R.; Mokhtarani, B. *Polym. Plast. Technol. Eng.*, **2016**, *56*, 543–555.
- Paulchamy, B.; Arthi, G.; Lignesh, B. D.; *J. Nanomed. Nanotechnol.*, **2015**, *6*, 1–4.
- Daas, B. M.; Ghosh, P. K.; Ghosh, S. *Indian J. Sci. Technol.*, **2017**, *10*, 1–11.
- Youh, M. J.; Huang, Y. R.; Peng, C. H.; Lin, Y. M.; Pu, N. W.; Liu, B. Y.; Chou, C. H.; Hou, K. H.; Gen, M. D. *Nanomaterials.*, **2021**, *11*.
- Zhang, Y.; Zhao, M.; Zhang, J.; Shao, Q.; Li, J.; Li, H.; Lin, B.; Yu, M.; Chen, S.; Guo, Z. *J. Polym. Res.*, **2018**, *25*, 130.
- Liu, X.; Chen, L.; Liu, Z.; Song, Q.; Liu, C. *Nanotechnol. Rev.*, **2021**, *10*, 1236–1252.
- Parhizkar, N.; Shahrabi, T.; Ramezanzadeh, B. *Eval. Program Plann.*, **2017** doi:10.1016/j.corsci.2017.04.011.
- Yang, Z.; Wang, L.; Sun, W.; Li, S.; Zhu, T.; Liu, W.; Liu, G.; *Appl. Surf. Sci.*, **2017**, *401*, 146–155.
- Li, A.; Chen, S.; Ma, Z.; Sun, M.; Zhu, G.; Zhang, Y.; Wang, W.; *Diam. Relat. Mater.*, **2021**, *116*, 108397.
- Ziat, Y.; Hammi, M.; Zahrri, Z.; Laghlimi, C. *J. Alloys Compd.*, **2020**, *820*, 153380.
- Saria, M.G.; Shamshiria, M.; Ramezanzadeh, B.; *Corr. Sci.*, **2017**, *129*, 38-53.

30. Liu, S.; Gu, L.; Zhao, H.; Chen, J.; Yu, H.; *J. Mater. Sci and Tech.*, **2019**, *32*, 425-431.
31. Niknahad, M.; Moradian, S.; Mirabedini, S.M., *Corros. Sci.*, **2010**, *52*, 1948-1952.
32. Yuan, T. H.; Zhang, Z. H.; Li, J.; Zhang, D. Q.; Gao, L. X.; Li, W. A.; Fan, Z. F. *Mater. Corros.*, **2019**, *1-8*, doi: 10.1002/maco.201810549.
33. Wierzbicka, E. ; Vaghefinazari, B. Lamaka, S.V. Zheludkevich, M. L.; Mohedano, M.; Moreno, L.; Visser, P.; Rodriguez, A.; Velasco, J.; Arrabal, R.; Matykina, E. *Corros. Sci.*, **2021**, *180*, 109-189.
34. Zhang, K.; Jiami, B.; Lua, b.; Li. J.; Zhanga, D.; Gao, L.; Zhou. H. *Corros. Sci.*, **2020**, *164*, 108352.
35. Izadi, M.; Shahrabi, T.; Ramezanzadeh, B. *Appl. Surf. Sci.*, **2018**, *440*, 491–505.
36. Zhang, Y.; Ye, H.; Liu, H.; Han, K.; *Corros. Sci.*, **2011**, *53*, 1694–1699.
37. Nikpour, B.; Ramezanzadeh, B., Bahlakeh, G.; Mahdavian, M. *Corros. Sci.*, **2017**, *127*, 240-259.
38. Zheng, A. H.; Shao, Y.; Wang, Y.; *Eval. Program Plann.*, **2017** doi:10.1016/j.corsci.2017.04.019.
39. Mohammed Ali Al-Sammarraie, A.; Hasan Raheema, M. *Int. J. Corros.*, **2017**, 1–9 .
40. Arouche, M. M.; Budhe, S.; Banea, M. D.; de Freitas, T. S.; de Barros, S., *Proc. Inst. Mech. Eng. Part L J. Mater. Des. Appl.*, **2019**, *233*, 1555–1563.